A Phase-Shifting MPPT Method to Mitigate Interharmonics from Cascaded H-Bridge PV Inverters

Pan, Yiwei; Sangwongwanich, Ariya; Yang, Yongheng; Blaabjerg, Frede

Published in:
Proceedings of 2020 IEEE Applied Power Electronics Conference and Exposition (APEC)

DOI (link to publication from Publisher):
10.1109/APEC39645.2020.9124258

Publication date:
2020

Document Version
Accepted author manuscript, peer reviewed version

A Phase-Shifting MPPT Method to Mitigate Interharmonics from Cascaded H-Bridge PV Inverters

Yiwei Pan, Ariya Sangwongwanich, Yongheng Yang, and Frede Blaabjerg
Department of Energy Technology, Aalborg University
Pontoppidanstraede 111, Aalborg DK-9220, Denmark
Email: {ypa, ars, yoy, fbl}@et.aau.dk

***Abstract*—Interhamonics are an emerging issue in photovoltaic (PV) systems. It has been revealed in the previous studies that the maximum power point tracking (MPPT) control is one of the responsibilities for interharmonic emissions. In cascaded H-bridge (CHB) PV inverters, if the MPPT perturbations of CHB cells are in-phase, the sum of the voltages of all CHB cells will oscillate with a higher amplitude, leading to large interharmonics in the grid. To address this, a phase-shifting MPPT method is proposed in this paper. By properly shifting the phase of the MPPT perturbation of each CHB cell, the oscillation of the equivalent total DC voltage can be effectively mitigated, and in turn, the interharmonics can be suppressed to a large extent. A 4-cell CHB PV inverter is examplified to demonstrate the proposed phase-shifting MPPT method, and *n*-cell CHB PV inverters have further been discussed regarding the implementation and control performances. The results have validated the effectiveness of the proposed method in terms of interharmonic suppression.**

***Keywords*—Interharmonics, cascaded H-bridge (CHB), maximum power point tracking (MPPT), photovoltaic (PV) systems.**

I. INTRODUCTION

With the growing installation of PV systems, challenging issues related to power quality are emerging [1]. For example, interharmonics have become one recently due to the large-scale adoption of power electronics [2]-[8]. As observed in laboratory tests [2], [3] and field measurements [4], [5], PV inverters potentially contribute to interharmonics, which may induce voltage fluctuation, flickering and unintentional disconnection [6]. Therefore, as recommended by IEC TS 63102 recently [7], interharmonics are considered as one of the assessment criteria for the grid-connected PV systems. It thus calls for cost-effective strategies to mitigate interharmonics. In the literature, it has also been revealed that the MPPT perturbation is one reason for interharmonic emissions [2]−[6]. Experimental results on a 3-kW single-phase grid-connected PV system are shown in Fig. 1 to demonstrate this phenomenon. It is further explained as follows: the low-frequency oscillation due to the MPPT will interact with the grid fundamental frequency through the control and interharmonics are then generated [2]. Nevertheless, the analysis, modeling, and mitigation of interharmonics from PV inverters was mainly on a two-level PV inverter.

This work was supported by the China Scholarship Council (CSC).

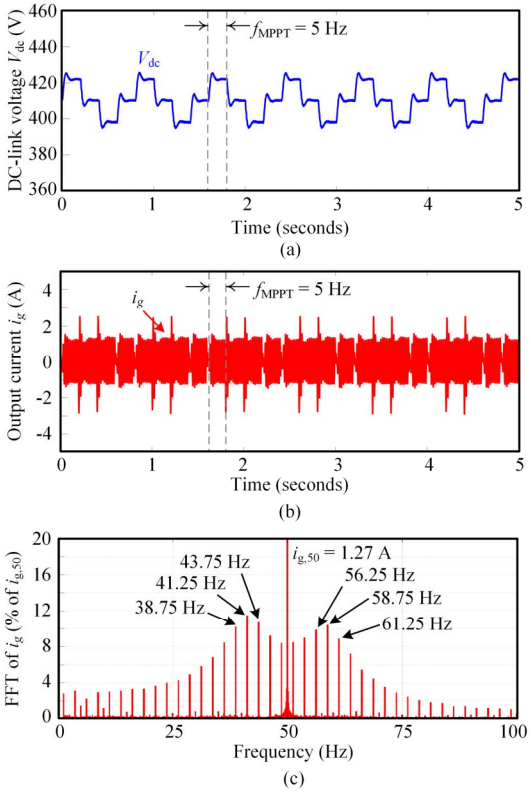

Fig. 1. Experimental results of a 3kW PV inverter operated at 10% of the rated power in a steady-state MPPT operation (MPPT sampling rate f_{MPPT} = 5 Hz, the perturbation step size v_{step} = 12 V) [6]: (a) filtered DC-link voltage, (b) grid current, and (c) frequency spectrum of the grid current.

In a large-scale PV system, the cascaded H-bridge (CHB) configuration has been introduced due to its modularity, high efficiency, and lower harmonics [9]−[13]. The overall diagram of the CHB PV inverter is shown in Fig. 2. According to the previous exploration, the MPPT perturbation for each CHB will inevitably generate interharmonics. As a consequence, if the DC-side oscillations of CHB cells are in-phase, the harmonics (interharmonics) of the total output currents will be magnified. This is explained that the equivalent total DC voltage (sum of the voltages of all CHB cells) will introduce large interharmonics. In other words, the interharmonic issue is much severer in the CHB PV inverter than one single

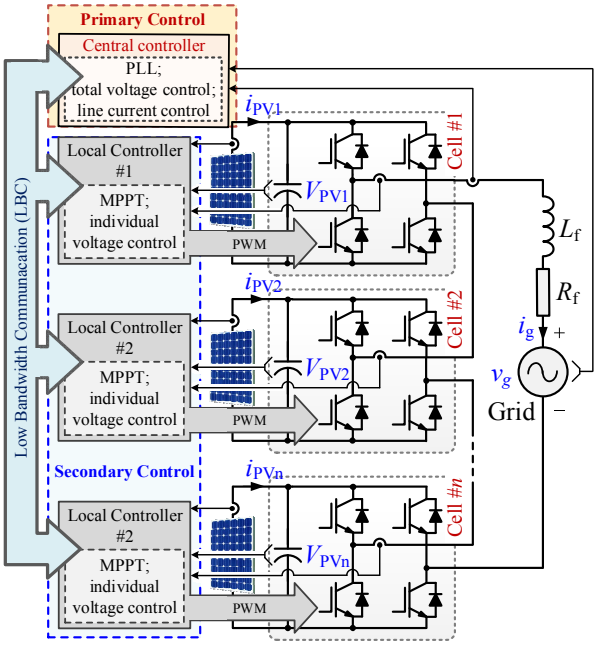

Fig. 2. Overall diagram of a single-phase CHB PV inverter.

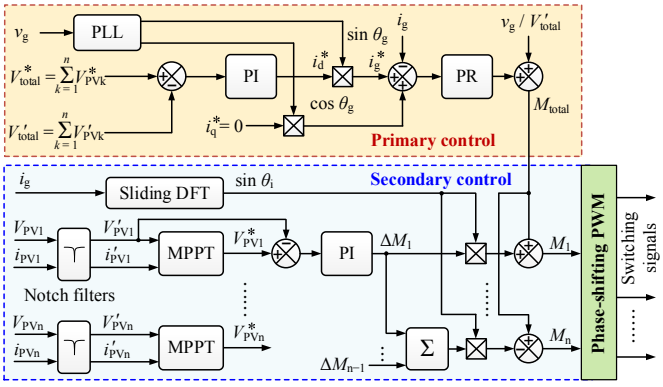

Fig. 3. Control diagram of a single-phase CHB PV inverter.

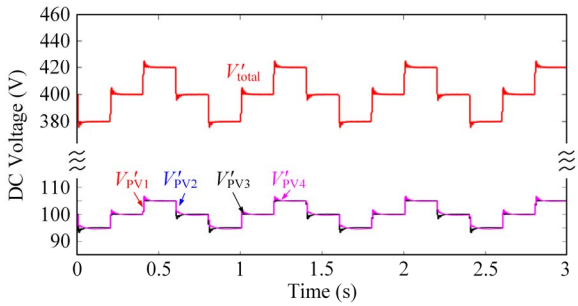

Fig. 4. Steady-state waveforms of the filtered DC voltages of the CHB PV inverter, operated at 100 W/m^2 and 25°C with in-phase MPPT voltage reference.

TABLE I
PARAMETERS OF THE CHB PV INVERTER

Rated power for one PV module	214 W
DC link capacitor	1000 μF
Grid-side L-filter	5 mH
Switching frequency of one cell	5 kHz
Controller sampling frequency	10 kHz
Grid voltage (RMS)	220 V
Grid Frequency	50 Hz
MPPT sampling rate	5 Hz
MPPT step-size	5 V

inverter. However, this issue has not been addressed in previous studies.

To alleviate the interharmonics, the sampling rate of the MPPT algorithm should be reduced, as suggested in [2]. However, this will lead to slow dynamics. In [6], a random sampling rate MPPT method was proposed to mitigate interharmonics in the single-phase two-level PV inverter. Nevertheless, its mitigation capability is limited, since the power oscillation of the MPPT still exists, which is the main source of interharmonics. On the other hand, the distributed DC-side of the CHB topology offers more control flexibility for the MPPT, which can potentially improve the inter-harmonics mitigation.

In this paper, a phase-shifting MPPT method is proposed for the CHB-based PV systems to tackle the interharmonics issue. By properly adjust the phase-shift between the MPPT perturbation of each CHB cell, the power oscillation at the DC-side can be minimized, and thereby the interharmonics. This concept is very similar with the phase-shifting method in motor drive applications in [14]. The rest of this paper is organized as follows. In Section II, the two-layer control structure of the CHB PV inverter is briefly introduced, as well as the particular interharmonic magnification issue in the CHB PV inverter. Then, the proposed phase-shifting MPPT method is detailed discussed in Section III. In Section IV, the effectiveness of the proposed method is verified by simulations on 3-cell and 4-cell CHB PV inverters. Finally, comcluding remarks are provided in Section V.

II. CONTROL STRUCTURE OF THE CHB PV INVERTER

The CHB-PV inverter is shown in Fig. 2, where the decentralized control is achieved with a two-layer structure. The primary control and the secondary control are located in the central controller and distributed in the local controllers, respectively, as shown in Fig. 3 [10], [13]. The primary control obtains the filtered voltage V'_{PVk} and voltage reference V^*_{PVk} (k denotes for the index of CHB cells) from all the local controllers through low-bandwidth communication (LBC). It also regulates the total DC voltage V'_{total} according to the sum of the MPPT voltage references V^*_{total} through a voltage proportional integral (PI) regulator, which generates the active current reference i^*_{d}. By multiplying i^*_{d} with the sine value of the grid voltage phase θ_{g}, the grid current reference i^*_{g} can be calculated. Then, the grid current i_{g} is regulated according to the current reference by a proportional resonant (PR) controller, giving the modulation index M_{total} which is equally distributed to each CHB cell. The secondary control is

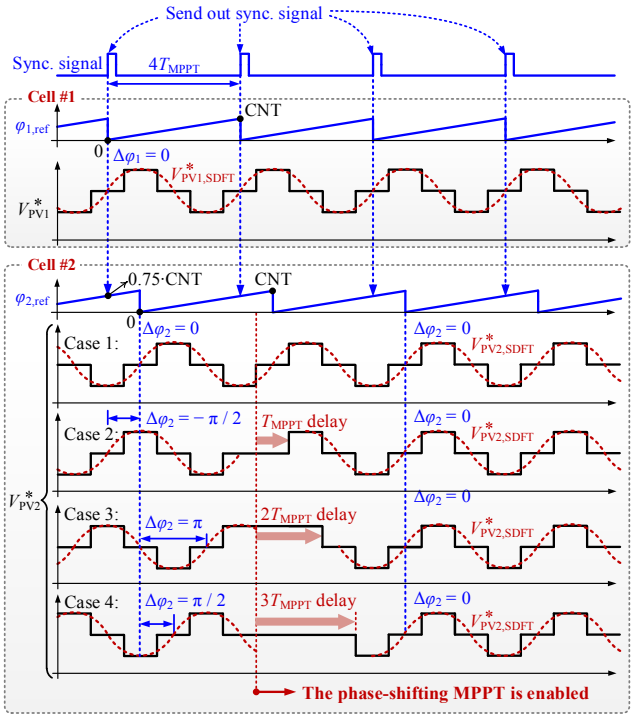

Fig. 5. Schematic diagram of the phase-shifting MPPT for cell #1 and #2 of a 4-cell CHB inverter.

responsible for the individual MPPT control, which is achieved by regulating independent PV voltages. As shown in Fig. 3, the individual PV voltage reference V^*_{PVk} is generated by the MPPT controller. In this paper, the Perturb and Observe (P&O) MPPT algorithm is employed. The DC voltage of each CHB cell is then regulated according to V^*_{PVk} through a PI regulator, which generate a modified value ΔM_k. The modulation index for the k^{th} CHB cell can be calculated by

$$M_k = M_{total} + \Delta M_k \sin\theta_i \tag{1}$$

where θ_i is the phase angle of the line current i_g, which is extracted by using the sliding discrete Fourier transform (SDFT) method [13], [15]. For the last CHB cell (the n^{th} cell), the modulation index should be calculated by

$$M_n = M_{total} - \left(\sum_{k=1}^{n-1} \Delta M_k\right) \sin\theta_i \tag{2}$$

With the above mentioned two-layer control method, the module-level MPPT can achieved for the CHB inverter, enabling harvesting more energy [10], [11].

In steady-state, the DC voltage of the PV panel varies around the maximum power point (MPP) [8]. If the DC voltage oscillation of each cell is in-phase, the oscillation amplitude of the equivalent total DC voltage will be n times larger than the P&O perturbation step-size (n denotes the number of CHB cells). To demonstrate this issue, a steady-state operation of a 4-cell CHB PV inverter is shown in Fig. 4, where the MPPT perturbations of all CHB cells are in-phase. The parameters of the CHB inverter are shown in Table I, and 4 series PV modules are interfaced to the DC bus of each CHB cell. As shown in Fig. 4, the equivalent total DC voltage oscillates with an amplitude of 20 V, which is 4 times larger than the oscillation on one CHB cell. This amplified oscillation will consequently lead to larger inter-harmonics in the grid current, and thus, efforts must be made to address this issue.

III. Proposed Phase-Shifting MPPT Control

The principle of the phase-shifting MPPT control is to properly adjusting (i.e., shifting) the phase of each three-stair DC voltage reference of the MPPT control in a way to minimize the overall oscillation of the equivalent total DC voltage. An example of the proposed method applied to a 4-cell CHB inverter is shown in Fig. 5, where only V^*_{PV1} and V^*_{PV2} are provided for illustration. As shown in Fig. 5, $\varphi_{1,ref}$ and $\varphi_{2,ref}$ are the phase-angle reference of cell #1 and #2, and $\varphi_{2,ref}$ is phase-shifted by $\pi/2$ in respect to $\varphi_{1,ref}$. The periods of these phase angle references equal to $4T_{MPPT}$, where T_{MPPT} denotes for the MPPT control period. Similarly, the phase references for cell #3 and #4, should be phase-shifted by π and $3\pi/2$ (or $-\pi/2$) in respect to $\varphi_{1,ref}$. These phase-shifted references can be realized by time-counters counting from 0 to CNT (the maximum value of time-counters) with different initial values. More specifically, the initial values for $\varphi_{1,ref}$, $\varphi_{2,ref}$, $\varphi_{3,ref}$ and $\varphi_{4,ref}$ are 0, 0.75·CNT, 0.5·CNT and 0.25·CNT. To synchronize these waveforms, a positive pulse is generated every $4T_{MPPT}$. This synchronization signal can be generated in the central controller or in any one of the local controllers, and sent out to all the cells through the serial communication system [16]. When the rise-edge of the synchronization signal is received by each cell, the initial value of each counter is forced to be loaded. In this way, a set of phase-shifted phase-angle reference can be realized.

With these phase-shifted phase angle references, the difference between the phase angle reference and the phase of the three-stair voltage can be calculated by

$$\Delta\varphi_k = \varphi_{k,ref} - \varphi_k \tag{3}$$

where φ_k denotes for the phase angle of the three-stair voltage reference for cell #k, and it can be obtained through the SDFT algorithm [15], which features a very simple structure for digital implementation with a sliding window and several addition and multiplication operations. To extract the actual phase of the three-stair voltages, the fundamental frequency of the SDFT should be set as $f_{MPPT}/4$, where f_{MPPT} refers to the MPPT frequency, and equals to $1/T_{MPPT}$. Due to the slow dynamics of the MPPT, the SDFT frequency is not very high. For example, $100{\cdot}f_{MPPT}$ can be enough. The fundamental component of the three-stair voltage for cell #k, denoted as $V^*_{PVk,SDFT}$, is also depicted in Fig. 5.

Depending on $\Delta\varphi_k$, a time delay is then inserted to realize the phase-shifting of the three-stair voltage. For instance, as shown in Fig. 5, before the enable of the phase-shifting MPPT control, there are four possible cases of oscillation for cell #2 with different phase angles, which are $\Delta\varphi_k = 0$, $-\frac{1}{2}\pi$, π and $\frac{1}{2}\pi$. Regarding these four cases, after the enable of the phase-

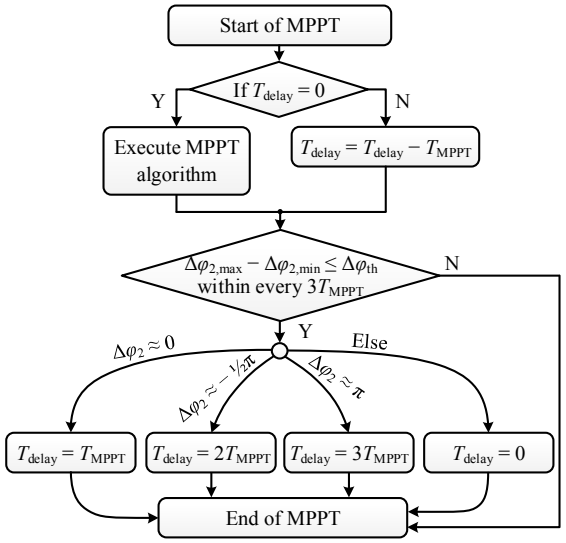

Fig. 6. Flowchart of the phase-shifting MPPT method for CHB cell #2.

shifting control, four types of time delay are inserted in each case, which are 0, T_{MPPT}, $2T_{MPPT}$ and $3T_{MPPT}$, respectively. In this way, during steady state, $\Delta\varphi_k$ can be controlled as 0, and the phase-angle of the voltage oscillation on each cell can be synchronized with the phase reference.

The flowchart of the phase-shifting MPPT method for cell #2 is shown in Fig. 6. As it can be observed in Fig. 6, after the start of the MPPT, if the inserted time delay T_{delay} equals to zero, the conventional MPPT algorithm is executed. Otherwise T_{delay} will be decreased by T_{MPPT}. Subsequently, if the difference between the maximum and minimum value of $\Delta\varphi_2$ is less than a small threshold $\Delta\varphi_{th}$ within three consecutive MPPT periods, cell #2 is regarded being operating in the steady state of MPPT, where its DC voltage reference is a three-stair waveform. In this condition, depending on the value of $\Delta\varphi_2$, four different values are assigned to T_{delay}. On the other hand, if $(\Delta\varphi_{2,max} - \Delta\varphi_{2,min})$ is beyond the range of $[-\Delta\varphi_{th}, \Delta\varphi_{th}]$, it is assumed that cell #2 is not operating in the three-stair voltage mode, and no changes will be made in terms of the delay T_{delay}. In the following MPPT periods, if T_{delay} is not zero, the conventional MPPT algorithm will be skipped until T_{delay} is reduced to zero after several MPPT periods. In this manner, the phase angle of the voltage oscillation can be kept consistent with the phase reference.

In the above discussion, the 4-cell CHB is employed to illustrate the proposed method. For *n*-cell CHB PV inverters, one set of inserted time delay values are shown in Table II. It should be mentioned that when even number of converter cells are cascaded, the oscillation in the equivalent total voltage can be fully eliminated. However, when the cascaded number of cells are odd, a small oscillation in the equivalent total voltage still exists. For instance, as shown in Table II, for the 3-cell CHB, the phase angle references for cell #1, #2 and #3 can be phase-shifted by 0, π/2 and π. In this case, the waveforms of the voltage references are shown in Fig. 7(a). As it can be observed from Fig. 7(a), the oscillation of cell #1 and #3 can be counteract with each other, while the DC voltage oscillation of cell #2 will inevitably emerge in the equivalent

TABLE II
PHASE SHIFT ANGLES OF *N*-CELL CHB PV INVERTERS

Cell index \ Total number of cells	2-cell	3-cell	4-cell	5-cell	6-cell	7-cell
Cell #1	0	0	0	0	0	0
Cell #2	π	π/2	π/2	π/2	π/2	π/2
Cell #3	/	π	π	π	π	π
Cell #4	/	/	3π /2	3π /2	3π /2	3π /2
Cell #5	/	/	/	0	0	0
Cell #6	/	/	/	/	π	π/2
Cell #7	/	/	/	/	/	π

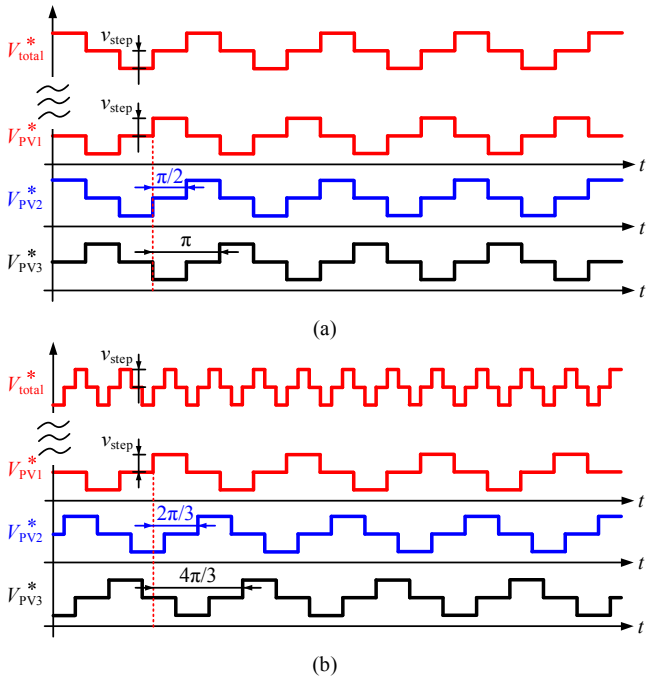

Fig. 7. Voltage references of the 3-cell CHB PV inverter with different sets of phase shift angles: (a) voltage reference for cell #1, #2 and #3 are phase shifted by 0, π/2 and π, and (b) voltage reference for cell #1, #2 and #3 are phase shifted by 0, 2π/3 and 4π/3.

total voltage reference. Even for other phase shift values, e.g., 0, 2π/3 and 4π/3 for cell #1, #2 and #3, the oscillation in the equivalent total voltage cannot be eliminated, as shown in Fig. 7(b). Nevertheless, despite this limitation, comparing to the in-phase oscillation case shown in Fig. 4, the proposed phase-shifting MPPT method is capable to reduce the oscillation in the equivalent total voltage by *n*-times for CHB with odd number of cells. Therefore, with the proposed method, interharmonics in the grid current can be effectively suppressed. When even-number of cells are cascaded, the suppression performance can be better.

Notably, the proposed phase-shifting method is only effective when the MPPT is operating in the steady-state. During the transient conditions such as the irradiance change, the steady-state criterion in Fig. 6 ($\Delta\varphi_{2,max} - \Delta\varphi_{2,min} \le \Delta\varphi_{th}$ within three consecutive T_{MPPT}) may not be satisfied, and the

conventional MPPT method will be executed. Therefore, the dynamic MPPT performance will not be affected by the proposed method. Although the oscillation of each DC voltage may not be properly phase-shifted during the transients, this is acceptable in practice, because the interharmonics are mainly introduced in the steady-state, when the equivalent total voltage oscillates with a frequency of $f_{MPPT}/4$.

IV. Simulation Results

In order to validate the effectiveness of the proposed method, simulations on 3-cell and 4-cell CHB PV inverters are performed in MATLAB/Simulink for odd and even number of cascading cases. The simulation results are shown in Figs. 8−13. The parameters of the simulation are shown in Table I.

Case 1: Firstly, the performance of the proposed method for a 3-cell CHB PV inverter is demonstrated under a constant irradiance condition (100 W/m^2), as shown in Fig. 8. Five series-connected PV modules were interfaced to each converter cell in the simulation, and the maximum power for each PV string is 1066 W. Before t = 10 s, the conventional MPPT is employed. In this case, the perturbations of the MPPT of all CHB cells are in-phase, as shown in Fig. 8. Accordingly, the equivalent total DC voltage oscillates with an amplitude of 15 V (e.g., three times higher than the individual perturbation step-size). Consequently, the grid current has a high amplitude of oscillations. As shown in Fig. 9(a), inter-harmonics appear in the grid current. The main interharmonics locates at 50 ± (2k + 1) · ($f_{MPPT}/4$) Hz [2], where k = 0, 1, 2…, and their amplitudes are around 0.04 A. When the proposed phase-shifting MPPT is enabled at t = 10 s, the oscillation of the equivalent total voltage V'_{total} is suppressed within 1 s (which is the required time for adjusting the phase-shifting). After t = 10.8 s, the amplitude of the oscillation on the equivalent total DC voltage is reduced to 5 V, which is three times smaller than the oscillation when the conventional MPPT control is applied. It can be seen from the individual PV panel voltage in Fig. 8(b) that the MPPT perturbation of cell #1, #2 and #3 are now phase-shifted by 0, π/2 and π, respectively. By doing so, the interharmonics of the grid current is reduced to one third, with the amplitude of the main interharmonics being 0.013 A, as shown in Fig. 9(b). Therefore, for the CHB PV inverter with odd number of cells, the interharmonics in the grid current can be effectively suppressed with the proposed method.

Case 2: The performance of the proposed method for a 4-cell CHB PV inverter under constant irradiance condition (100 W/m^2) is shown in Fig. 10. Each converter cell is interfaced with a string of 4 series-connected PV modules, and the maximum power is 856 W for each PV string. As it can be observed in Fig. 10, before t = 10 s, due to the in-phase perturbations on the DC voltages of all CHB cells, the oscillation in the equivalent total voltage reaches 20 V, i.e., 4 times larger than the oscillation on one CHB cell. Meanwhile, remarkable interharmonics appear on the grid current, as shown in Fig. 11(a), with the main interharmonics locating at 50 ± (2k + 1) · ($f_{MPPT}/4$), and their amplitudes are around 0.05 A. When the proposed phase-shifting MPPT method is

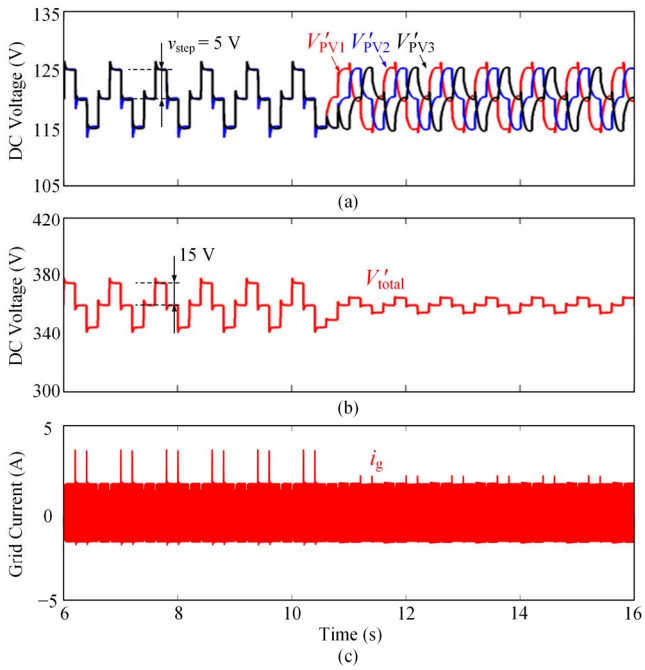

Fig. 8. Simulation results of a 3-cell CHB PV inverter operated at 100 W/m^2 and 25°C, with phase-shifting MPPT control enabled at 10 s: (a) DC voltages of 3 CHB cells, (b) the equivalent total DC voltage, (c) grid current.

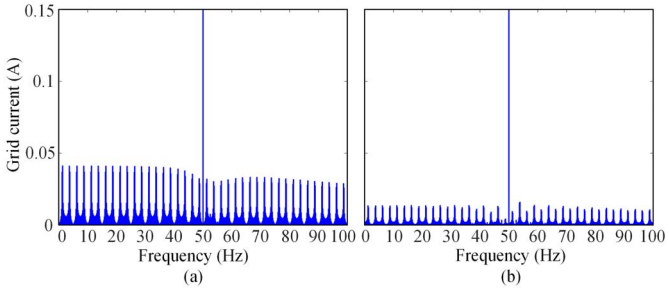

Fig. 9. Frequency spectrums of the grid current i_g shown in Fig. 8: (a) with in-phase MPPT perturbations and (b) with the proposed phase-shifting MPPT control.

enabled at t = 10 s, the MPPT perturbation of each cell #1−4 is phase-shifted by 0, π/2, π and 3π/2 after 5 MPPT cycles. Compared to Case 1, the oscillation in the equivalent total voltage is fully eliminated in the 4-cell CHB inverter. Thus, the interharmonics are almost fully suppressed, as it is shown in Fig. 11(b). Most interharmonics are below 0.005 A, except the interharmonics at 50 ± 1.25 Hz and 50 ± 3.75 Hz, whose amplitudes are only 0.02 A and 0.007 A. Therefore, for the CHB PV inverters with an even number of cascaded cells, the oscillation in the equivalent total voltage can be fully eliminated by the proposed phase-shifting MPPT method, resulting an even better interharmonic suppression performance compared to the case with an odd number of cascaded cells.

Case 3: To verify the performance of the proposed method under irradiance changes, simulations are carried out on the 4-cell CHB PV inverter and the results are provided in Fig. 12. In this case, the irradiance level for PV1, PV3 and PV4 jumps from 100 W/m^2 to 300 W/m^2 at t = 20 s, and the irradiance for

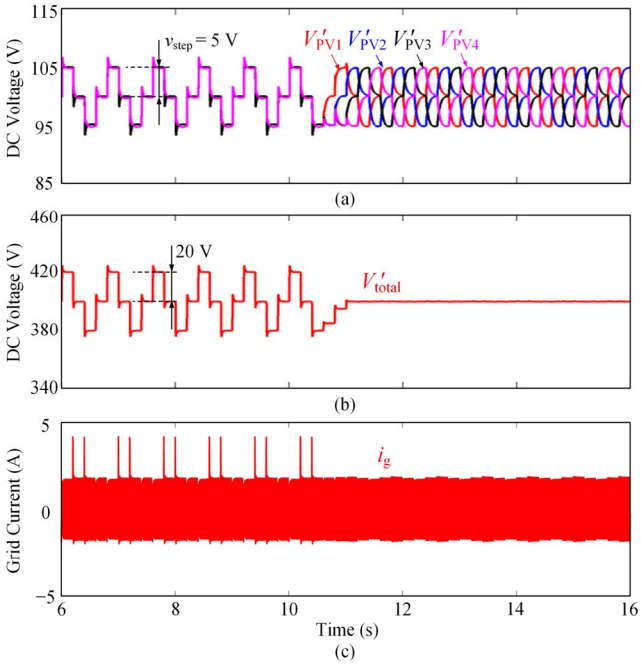

Fig. 10. Simulation results of a 4-cell CHB PV inverter operated at 100 W/m^2 and 25°C, with phase-shifting MPPT control enabled at 10 s: (a) DC voltages of 4 CHB cells, (b) the equivalent total DC voltage, (c) grid current.

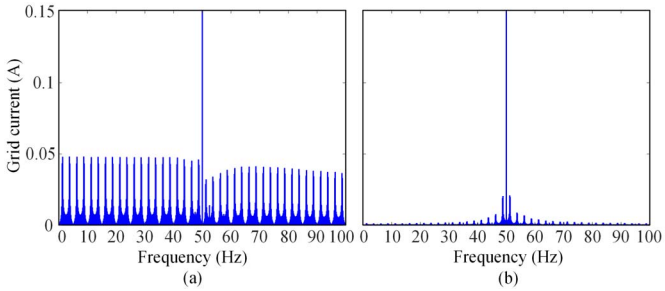

Fig. 11. Frequency spectrums of the grid current i_g shown in Fig. 10: (a) with in-phase MPPT perturbations and (b) with the proposed phase-shifting MPPT control.

PV2 changes from 100 W/m^2 to 250 W/m^2 at the same time. As it is seen in Fig. 12, during 20 s to 23 s, PV1, PV2, PV3 and PV4 enter the steady-state at t = 23 s, 22.4 s, 23 s and 21.6 s, respectively. During this transition, the oscillation can be observed on the equivalent total voltage as the phase-shift of each cell is being adjusting in this period. After 23 s, all the DC voltages are properly phase-shifted, and no oscillation can be observed in the equivalent total voltage V'_{total}. Consequently, the interharmonics are still low on the grid current i_g, as shown in Fig. 13.

V. Conclusions

In the CHB PV inverter, the oscillation in the equivalent total voltage may be amplified, if the MPPT perturbations of all CHB cells are in-phase. This can lead to larger inter-harmonics in the grid current when the conventional MPPT control is employed. To tackle this issue, a phase-shifting MPPT method for the CHB PV inverter has been proposed in this paper. The proposed method shifts the phase of the MPPT

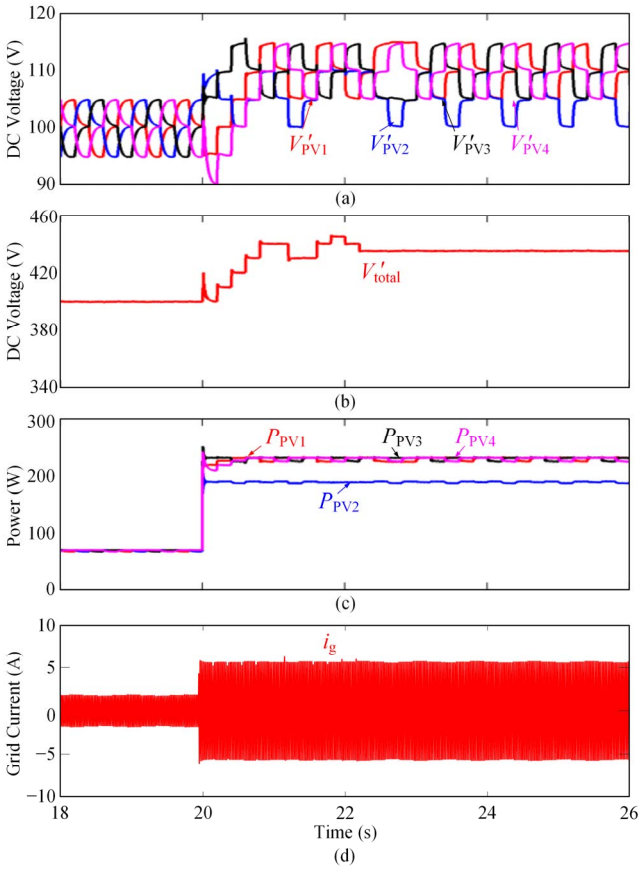

Fig. 12. Performance of the phase-shifting MPPT method under PV irradiance change: (a) DC voltages of 4 CHB cells, (b) the equivalent total DC voltage, (c) PV power of 4 CHB cells, and (d) grid current.

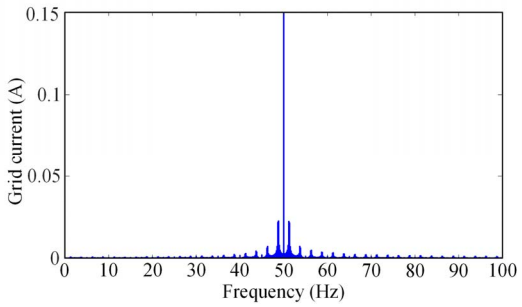

Fig. 13. Frequency spectrums of the grid current i_g shown in Fig. 12 after 23s.

perturbation of each CHB cell in a way to counteract with each other. By doing so, the oscillation of the equivalent total voltage can be suppressed, and the interharmonics can be significantly reduced, especially when an even number of cells are employed in the CHB, while maintaining the MPPT performance. This method is very simple for implementation, and can be easily expanded to n-cell CHB PV inverters.

References

[1] *IEEE Standard for Interconnection and Interoperability of Distributed Energy Resources with Associated Electric Power Systems Interfaces*, IEEE Standard 1547-2018, Apr. 2018.

[2] A. Sangwongwanich, Y. Yang, D. Sera, H. Soltani, and F. Blaabjerg, "Analysis and modeling of interharmonics from grid-connected photovoltaic systems," *IEEE Trans. Power Electron.*, vol. 33, no. 10, pp. 8353-8364, Oct. 2018.

[3] R. Langella, A. Testa, J. Meyer, F. Mller, R. Stiegler, and S. Z. Djokic, "Experimental-based evaluation of PV inverter harmonic and interharmonic distortion due to different operating conditions," *IEEE Trans. Instrum. Meas.*, vol. 65, no. 10, pp. 2221–2233, Oct. 2016.

[4] V. Ravindran, S. K. Rnnberg, T. Busatto, and M. H. J. Bollen, "Inspection of interharmonic emissions from a grid-tied PV inverter in north Sweden," in *Proc. Int. Conf. Harmonics Quality Power*, pp. 1–6, May 2018.

[5] V. Ravindran, T. Busatto, S. K. Ronnberg, J. Meyer, and M. Bollen, "Time-varying interharmonics in different types of grid-tied PV inverter systems," *IEEE Trans. Power Del*., DOI: 10.1109/TPWRD.2019. 2906995.

[6] A. Sangwongwanich and F. Blaabjerg, "Mitigation of interharmonics in PV systems with maximum power point tracking modification," *IEEE Trans. Power Electron*., vol. 34, no. 9, pp. 8279-8282, Sept. 2019.

[7] *Grid code compliance assessment methods for grid connection of wind and PV power plants*, Ed. 1, IEC/TS 63102, 2016.

[8] Y. Yang, K. A. Kim, F. Blaabjerg, and A. Sangwongwanich, *Advances in Grid-Connected Photovoltaic Power Conversion Systems*, Publisher: Woodhead Publishing, 2018.

[9] X. Zhang, T. Zhao, W. Mao, D. Tan, and L. Chang, "Multilevel inverters for grid-connected photovoltaic applications: examining emerging trends," *IEEE Power Electron. Mag*., vol. 5, no. 4, pp. 32-41, Dec. 2018.

[10] E. Villanueva, P. Correa, J. Rodriguez, and M. Pacas, "Control of a single-phase cascaded H-bridge multilevel inverter for grid-connected photovoltaic systems," *IEEE Trans. Ind. Electron*., vol. 56, no. 11, pp. 4399-4406, Nov. 2009.

[11] B. Xiao, L. Hang, J. Mei, C. Riley, L. M. Tolbert, and B. Ozpineci, "Modular cascaded H-bridge multilevel PV inverter with distributed MPPT for grid-connected applications," *IEEE Trans. Ind. Appl*., vol. 51, no. 2, pp. 1722-1731, Mar./Apr. 2015.

[12] L. Du and J. He, "A simple autonomous phase-shifting PWM approach for cascaded H-Bridge converters," *IEEE Trans. Power Electron*., vol. 34, no. 12, pp. 11516-11520, Dec. 2019.

[13] Y. Pan, C. Zhang, S. Yuan, A. Chen and J. He, "A decentralized control method for series connected PV battery hybrid microgrid," in *Proc. IEEE Transp. Electrific. Conf. Expo, Asia-Pacific (ITEC Asia-Pacific)*, Harbin, China, Aug. 2017, pp. 1–6.

[14] Y. Yang, P. Davari, F. Zare, and F. Blaabjerg, "A DC-link modulation scheme with phase-shifted current control for harmonic cancellations in multidrive applications," *IEEE Trans. Power Electron.*, vol. 31, no. 3, pp. 1837-1840, Mar. 2016.

[15] E. Jacobsen and R. Lyons, "The sliding DFT," *IEEE Signal Process. Mag*., vol. 20, no. 2, pp. 74–80, Mar. 2003.

[16] Y. M. Park, J. Y. Yoo, and S. B. Lee. "Practical implementation of PWM synchronization and phase-shift method for cascaded H-bridge multilevel inverters based on a standard serial communication protocol," *IEEE Trans. Ind. Appl*., vol. 44, no. 2, pp. 634-643, Mar./Apr., 2008.